Superoxide dismutase and pseudocatalase increase tolerance to Hg(II) in *Thermus thermophilus* HB27 by maintaining the reduced bacillithiol pool.

Javiera Norambuena[1], Thomas E. Hanson T[2], Tamar Barkay[1*], Jeffery M. Boyd[1*]

[1]Department of Biochemistry and Microbiology, Rutgers University, New Brunswick, New Jersey, USA.

[2]School of Marine Science and Policy, Delaware Biotechnology Institute, and Department of Biological Sciences, University of Delaware, Newark, Delaware, USA.

*To whom correspondence may be addressed: Jeffrey M. Boyd or Tamar Barkay, Department of Biochemistry and Microbiology, Rutgers University, 76 Lipman Drive, New Brunswick, New Jersey, 08901, Telephone: (848) 932-5604, E-mail: jeffboyd@SEBS.rutgers.edu (JB) or Telephone: (848) 932 5664, E-mail: tamar.barkay@rutgers.edu (TB).

Running title: Running title: Bacillithiol, ROS, and mercury resistance

ABSTRACT

Mercury (Hg) is a widely distributed, toxic heavy metal with no known cellular role. Mercury toxicity has been linked to the production of reactive oxygen species (ROS), but Hg does not directly perform redox chemistry with oxygen. How exposure to the ionic form, Hg(II), generates ROS is unknown. Exposure of *T. thermophilus* to Hg(II) triggered ROS accumulation and increased transcription and activity of superoxide dismutase (Sod) and pseudocatalase (Pcat); however, Hg(II) inactivated Sod and Pcat. Strains lacking Sod or Pcat had increased oxidized bacillithiol (BSH) levels and were more sensitive to Hg(II) than the wild type. The Δ*bshA* Δ*sod* and Δ*bshA* Δ*pcat* double mutant strains were as sensitive to Hg(II) as the Δ*bshA* strain that lacks bacillithiol, suggesting that the increased sensitivity to Hg(II) in the Δ*sod* and Δ*pcat* mutant strains is due to a decrease of reduced BSH. Treatment of *T. thermophilus* with Hg(II) decreased aconitase activity and increased the intracellular concentration of free Fe and these phenotypes were exacerbated in Δ*sod* and Δ*pcat* mutant strains. Treatment with Hg(II) also increased DNA damage. We conclude that sequestration of the redox buffering thiol BSH by Hg(II), in conjunction with direct inactivation of ROS scavenging enzymes, impairs the ability of *T. thermophilus* to effectively metabolize ROS generated as a normal consequence of growth in aerobic environments.

IMPORTANCE

Thermus thermophilus is a deep-branching thermophilic aerobe. It is a member of the Deinococcus-Thermus phylum that, together with the Aquificae, constitute the earliest branching aerobic bacterial lineages; therefore, this organism serves as a model for early-

diverged bacteria (1) whose natural heated habitat may contain mercury of geological origins (2). *T. thermophilus* likely arose shortly after the oxidation of the biosphere 2.4 billion years ago. Studying *T. thermophilus* physiology provides clues about the origin and evolution of mechanisms for mercury and oxidative stress responses, the latter being critical for the survival and function of all extant aerobes.

KEY WORDS: *Thermus thermophilus*, reactive oxygen species, mercury, thermophile, bacillithiol, superoxide dismutase, pseudocatalase, iron.

INTRODUCTION

All aerobes face oxidative stress, which occurs when the balance between pro-oxidants and antioxidants is tipped towards pro-oxidants. Reactive oxygen species (ROS) are pro-oxidants that are produced by reduction of dioxygen. This can happen intracellularly through the interaction of dioxygen with reduced flavin prosthetic groups (3). The transfer of one- or two-electrons to dioxygen produces superoxide (O_2^-) and hydrogen peroxide (H_2O_2), respectively (4). A three-electron transfer catalyzed by redox active divalent transition metals, such as copper and iron (Fe) via Fenton and Haber-Weiss reactions, can produce hydroxyl radicals ($^{\bullet}OH$). These radicals are short-lived and rapidly react with multiple cellular constituents including DNA (4).

Mercury (Hg) does not perform redox chemistry under biological conditions, but in animal models Hg(II) exposure results in oxidative stress (5-9). Increased ROS upon Hg(II) exposure is thought to result from the depletion of cellular redox buffers (5, 8, 10) and/or the inhibition of the electron transport chain allowing electrons to accumulate on flavoproteins (6, 8, 11). In bacteria, Hg(II) triggered the release of Fe(II) from solvent exposed iron sulfur (Fe-S) clusters (12). Oxidation of solvent accessible 4Fe-4S clusters by superoxide or H_2O_2 also results in Fe(II) release (13, 14). An increased pool of non-chelated or “free” cytosolic Fe(II) can accelerate Fenton chemistry (15).

Metabolic subsystems have evolved to detoxify Hg(II). Resistance to Hg(II) is encoded by the mercury resistance operon (*mer*), which is widely distributed over the bacterial and archaeal kingdoms (16). The gene composition of this operon varies among organisms, but all *mer* operons encode for the mercuric reductase (MerA), which reduces Hg(II) to elemental mercury. Elemental Hg is volatile and diffuses out of the cell. Many

74 *mer* operons also encode for Hg(II) sequestration and/or transport,and the Hg(II)-
75 responsive transcriptional regulator of the operon, MerR (16). Deeply branching microbes
76 have simple *mer* operons (17); the *T. thermophilus* operon is composed of *merA*, *merR*,
77 and *oah2*. The latter encodes a homolog of *O*-acetyl-homocysteine sulfhydrylase, an
78 enzyme normally involved in methionine biosynthesis and recycling (18, 19).

79 Our knowledge of the *mer* system comes from studies with the most derived taxa
80 including *Escherichia coli*, *Pseudomonas*, and *Bacillus*. *T. thermophilus* is a deep-
81 branching thermophilic organism that responds differently to Hg(II) exposure than *E. coli*
82 (19). It also possesses a different set of enzymes to detoxify ROS and it uses bacillithiol
83 (BSH) as the primary low molecular weight (LMW) thiol (19). *T. thermophilus* also
84 accumulates high concentrations of intracellular sulfides (324.1$\pm$ 88.4 nmol/g dry weight)
85 (19). Mercury has a high affinity for cellular thiols (20, 21) and exposure to 3 μM Hg(II)
86 completely depleted free BSH pools in *T. thermophilus* (19). Interestingly, the cellular
87 concentration of BSH is predicted to be an order of magnitude higher than the
88 concentration of Hg(II) that depleted the reduced BSH pool (presented herein and (19))
89 suggesting that sequestration of BSH by Hg(II) is only depleting a portion of the BSH pool.
90 These findings have led us to ask what happens to the rest of the BSH upon Hg(II)
91 challenge. The disturbance of thiol-containing redox buffers, which play critical roles in
92 ROS detoxification and oxidized protein repair, can lead to ROS accumulation (22). There
93 is not a clearly established connection between Hg(II) and ROS in microbes and even
94 less is known about physiologically diverse microbes like *T. thermophilus* that utilize
95 alternative redox buffers such as BSH.

We tested the overarching hypothesis that exposure of *T. thermophilus* to Hg(II) increases ROS accumulation because of decreased availability of reduced BSH. We demonstrate that Hg(II) exposure results in ROS accumulation. This is, in part, the result of Hg(II)-dependent inactivation of the ROS metabolizing enzymes superoxide dismutase (Sod) and pseudocatalse (Pcat). Strains lacking ROS metabolizing enzymes contain decreased levels of reduced BSH and display increased sensitivity to Hg(II). Hg(II) exposure also inactivated aconitase, which requires a solvent accessible Fe-S cluster, and increased free cytosolic Fe pools. This effect likely promotes ROS generation via Fenton chemistry, which we monitored by measuring DNA damage. Taken together, these findings confirm that an enzymatic capacity to detoxify ROS is important for the maintenance of a reduced intracellular thiol pool, which is necessary to mitigate Hg(II) toxicity in *T. thermophilus*.

RESULTS

Mercury exposure results in ROS accumulation and inactivates ROS-scavenging enzymes. We tested the hypothesis that Hg(II) exposure would increase ROS accumulation in *T. thermophilus*. After exposure to Hg(II), total intracellular ROS levels were qualitatively measured with the fluorescent probe 2',7'-dichlorodihydrofluorescein diacetate (H_2DCFDA). Exposure to 4 or 8 μM Hg(II) for 60 minutes resulted in a significant increase in DCFDA-based fluorescence suggesting increased ROS accumulation (Fig. 1A).

The genome of *T. thermophilus* encodes one manganese-dependent superoxide dismutase (Sod) to detoxify superoxide. It does not possess catalase, but instead,

encodes a nonheme catalase, or pseudocatalase (Pcat), that utilizes an active site manganese to metabolize H_2O_2 (23). It also possesses two types of peroxiredoxins: osmotically inducible protein (OsmC) and bacterioferritin comigratory protein (Bcp). These are members of the thiol peroxidase family, which catalyze the reduction of hydroperoxides (24, 25). The genome also encodes a thioredoxin-related protein, thiol:disulfide interchange protein (TlpA), which is involved in oxidative stress responses (26).

We tested the hypothesis that Hg(II) exposure increases the transcription of genes involved in ROS detoxification. Exposure of *T. thermophilus* to 1 μM Hg(II) increased transcript levels of *sod, pcat*, *osmC*, and *tlpA* (Fig. 1B). This induction was noted after 7.5 minutes (not shown) and sustained for at least 30 minutes after Hg(II) exposure (Fig. 1B). Only *bcp* transcript levels were not significantly changed. The strongest induction was observed after 15 min of Hg(II) exposure. The greatest induction was noted for *pcat*, which was induced 107±23-fold.

We next examined whether the increased transcription of *sod* and *pcat* would correlate with increased enzyme activity. Cells were exposed to Hg(II) for 30 min, and then H_2O_2 and superoxide (SOD) scavenging activities were measured in cell-free lysates. Hg(II) exposure significantly increased H_2O_2 consumption by approximately 2-fold. A Δ*pcat* mutant strain lost >90% of the H_2O_2 consumption activity suggesting that Pcat functions in H_2O_2 metabolism (Fig. 1C). Superoxide consumption appeared to increase relative to the unexposed control, but it was not statistically significant ($p=0.249$) (Fig. 1C). A Δ*sod* strain displayed 8-fold lower superoxide scavenging activity than the Hg(II)-unexposed parent, correlating superoxide consumption with the presence of Sod.

Comparing the transcript levels and enzymatic activities revealed a significant disconnect. Hg(II) exposure resulted in greatly increased *sod* and *pcat* transcript levels, without a commensurate increase in Sod and Pcat activities. We tested the hypothesis that Hg(II) exposure was detrimental to Sod and Pcat activities. We used *T. thermophilus* cell-free lysates generated from cells that had not been exposed to Hg(II). Incubation of the cell-free lysate with 100 μM Hg(II) resulted in a 70% decrease in Pcat activity (Fig. S1C). We were not able to conduct traditionally described SOD assays because xanthine oxidase was inhibited by Hg(II); therefore, we measured Sod and Pcat activities with zymography. When lysates were directly exposed to Hg(II) the activities of both Sod and Pcat were decreased (Figs. 1D and F). Gel-localized activities were verified using the Δ*sod* and Δ*pcat* strains (Figs. 1E and G). The Δ*sod* and Δ*pcat* strains were more sensitive to paraquat and H_2O_2, respectively (Fig. S1).

We examined whether Hg(II) affects Pcat and Sod *in vivo*. To this end, we stopped protein synthesis and incubated cells with and without 1 or 5 μM Hg(II) before H_2O_2 and superoxide consumption was monitored in cell-free lysates. In absence of Hg(II), Pcat and Sod activities were approximately 50% after 30-minute exposure to chloramphenicol, (533±26 and 3.9±0.3 U/mg protein, respectively). Exposure to 5 μM Hg(II) further decreased consumption of superoxide, by 25% (to 2.9±0.3 U/mg), and H_2O_2, by 15% (to 453±15 U/mg), when compared to the chloramphenicol only treated cells (Fig. 1H). Incubation with 1 μM Hg(II) did not result in a significant decrease in SOD or Pcat activities (not shown). These findings demonstrate that Hg(II) exposure resulted in ROS accumulation and increased activities of Pcat and Sod *in vivo*. However, the strong transcriptional induction of *pcat* and *sod* only translated into modest increases in Sod and

165 Pcat activities. This could be, in part, the result of Hg(II) inhibition of the holo-enzyme or
166 of enzyme maturation.
167
168 **Strains lacking superoxide- or H_2O_2-scavenging activities are more sensitive**
169 **to Hg(II).** We tested the hypothesis that Sod and Pcat have roles in mitigating Hg(II)
170 toxicity. When compared to the parent strain (WT), *T. thermophilus* Δ*sod* and Δ*pcat*
171 mutants had increased sensitivity to Hg(II) with 50% inhibitory concentrations (IC_{50}) of 2.5
172 μM and 3 μM, respectively (Figs. 2A and B). The WT IC_{50} for Hg(II) was 4.5 μM. The Δ*sod*
173 strain was as sensitive to Hg(II) as the Δ*merA* strain. Genetic complementation of the
174 Δ*sod* (Figs. S2A and C) and Δ*pcat* (Figs. S2B and D) strains verified that the lack of Sod
175 or Pcat was responsible for the observed phenotypes.
176 We tested the hypothesis that the roles of Sod or Pcat in mitigating Hg(II) toxicity
177 were independent of the function of MerA. We compared the Hg(II) sensitivities of the
178 Δ*merA* Δ*sod* and Δ*merA* Δ*pcat* double mutants to that of the Δ*merA* mutant. The double
179 mutant strains were more sensitive to Hg(II) than the Δ*merA* strain (Fig. 2C) suggesting
180 that the roles of Sod, Pcat, and MerA in Hg(II) resistance are independent and
181 complementary.
182 We next tested the corollary hypothesis that ROS accumulation would occur at
183 lower Hg(II) concentrations in the Δ*sod* and Δ*pcat* strains compared to the WT strain. We
184 were unable to detect ROS accumulation in the Δ*sod* and Δ*pcat* strains in the absence of
185 Hg(II) (Fig. 2D). ROS accumulation was noted in the Δ*sod* and Δ*pcat* strains upon
186 exposure to 0.5 and 2 μM Hg(II), whereas no change in ROS levels were noted in the WT

187 strain. These results led us to conclude that Sod and Pcat mitigate Hg(II) toxicity by
188 controlling ROS accumulation.
189
190 ***T. thermophilus*** **strains lacking Sod or Pcat contain smaller reduced BSH**
191 **pools.** We tested the hypothesis that BSH functions in metabolizing ROS or the
192 byproducts or ROS damage. We quantified the reduced BSH pools in the Δ*sod* and Δ*pcat*
193 strains by monobromobimane derivatization and HPLC, which quantifies free BSH pools.
194 Free BSH was undetectable in the Δ*sod* mutant (Fig. 3A) and the Δ*pcat* strain had 80%
195 less free BSH than the WT strain (7.2± 6.7 versus 33.2± 10.2 nmol g^{-1} dry weight for the
196 WT) (Fig. 3A). Importantly, all strains had approximately the same intracellular
197 concentration of total (reduced+oxidized) BSH (Fig. 3A) strongly suggesting that the lack
198 of free BSH is due to its oxidation in the mutant strains or defective recycling of bacillithiol
199 disulfide (BSSB) back to BSH. The same HPLC traces did not display a significant
200 difference in intracellular sulfide concentrations between the WT, Δ*sod*, and Δ*pcat* strains,
201 but these peaks were quite broad making it difficult to accurately quantify (data not
202 shown).
203 Reduced BSH is required to detoxify the antibiotic fosfomycin (27) and mitigate
204 oxidative stress (28). The Δ*sod* and Δ*pcat* strains were more sensitive to fosfomycin than
205 the WT and had fosfomycin sensitivities similar to that of the Δ*bshA* strain (Fig. 3B), which
206 cannot synthesize BSH (19). When compared to the WT strain, the Δ*bshA* strain showed
207 increased sensitivity to H_2O_2 and paraquat; however, the Δ*bshA* strain was less sensitive
208 to the toxicants than the Δ*sod* and Δ*pcat* strains (Fig. S1).

ROS-scavenging deficient strains were constructed in the Δ*bshA* background to test if Hg(II) sensitivity in the Δ*pcat* and Δ*sod* strains was exacerbated by a complete lack of BSH (19). The Hg(II) sensitivity phenotypes corresponding to the Δ*bshA* and Δ*pcat* mutations were not additive (Fig. 3C), but the Δ*sod* strain was more sensitive to 3 μM Hg(II) than the Δ*bshA* strain (Fig. 3D). These results suggested that Sod has a role in preventing Hg(II) toxicity in addition to its role in preventing the oxidation of BSH pool while the Hg(II) sensitivity of the Δ*pcat* strain appears to result from a lack of reduced BSH.

Hg(II) exposure results in decreased aconitase (AcnA) activity, increased free cytosolic Fe, and DNA damage. BSH plays a fundamental role in Hg(II) resistance in *T. thermophilus* and exposure to 3 μM Hg(II) completely depleted free BSH pools (19). The Δ*sod* and Δ*pcat* strains had decreased concentrations of reduced BSH (Fig. 3A) suggesting that there may be more free Hg(II) in the cytoplasms of the Δ*sod* and Δ*pcat* strains when challenged with Hg(II). Prior work in *E. coli* found that Hg(II) inactivated fumarase, which requires a solvent accessible Fe-S cluster for catalysis (12). When *T. thermophilus* was exposed to 1 μM Hg(II) for 30 minutes, AcnA activity decreased to 50% of the unexposed control (Fig. 4A). The non-challenged Δ*pcat* and Δ*sod* strains had 12 and 16% of the activity of the WT strain, respectively (Fig. 4A). Upon exposure to Hg(II), AcnA activity was reduced a further 30-fold in the Δ*sod* strain and 4.5-fold in the Δ*pcat* strain (Fig. 4A). We next examined whether Hg(II) inactivated *T. thermophilus* AcnA *in vitro*. To this end, we added Hg(II) to anaerobic cell-free lysates prior to measuring AcnA

activity. AcnA activity decreased as a function of Hg(II) added and was nearly undetectable after exposure to 100 μM Hg(II) (Fig. 4B).

We next tested the hypothesis that Hg(II)-exposure would increase the size of the cytosolic free Fe pool. *T. thermophilus* was exposed, or not, to 4 μM Hg(II) for 30 minutes and intracellular free Fe was quantified using electron paramagnetic resonance (EPR) spectroscopy (21, 29). Exposure significantly increased the pool of free Fe by 1.7-fold (Fig. 4C). When the WT, Δ*sod*, and Δ*pcat* strains were exposed to 0.25 μM Hg(II), the WT free Fe pool was unaltered while it was significantly increased, 1.8-fold, in the Δ*sod* and Δ*pcat* strains; however, at 4 μM Hg(II) the free Fe pool was elevated in the WT strain (Fig. 4C). Thus, treatment with a lower concentration of Hg(II) was capable of disrupting the Fe homeostasis in the Δ*sod* and Δ*pcat* strains when compared to the WT. These strains had similar free Fe levels when cultured in the absence of Hg(II) (Fig. 4C).

Free Fe(II) can catalyze Fenton chemistry to produce $HO^{\bullet}$ (4) that can damage DNA (30) by producing apurinic/apyrimidinic (AP) sites (31, 32). We hypothesized that Hg(II) exposure would result in increased DNA damage. After exposure to either 2 and 4 μM Hg(II) there was a significant increase in AP sites (Fig. 4D). Repair of AP sites requires base excision repair, which In *T. thermophilus* depends on the Nfo endonuclease IV (33). A *T. thermophilus* Δ*nfo* mutant was more sensitive to Hg(II) than the WT strain (Fig. S3).

Taken together these data are consistent with a model wherein Hg(II) exposure decreases the activities of enzymes requiring solvent exposed Fe-S clusters and increases intracellular free Fe. The increase in free Fe likely contributes to increased hydroxyl radicals resulting in increased DNA damage.

DISCUSSION

The mechanisms by which metals exert toxicity are not fully understood. These phenomena have largely been examined in model organisms and relatively few studies have been conducted in physiologically or phylogenetically diverse organisms. In this study, we examined the effect of Hg(II) exposure on a deeply branching thermophilic bacterium to expand our knowledge of Hg(II) toxicity and tolerance in phylogenetically and physiologically diverse microbes.

Data presented herein, and from our previous study (19), have led to a working model for how Hg(II) exposure affects *T. thermophilus* (Fig. 5). In our model, increased titers of cytosolic Hg(II) results in ROS accumulation, which also may be the result of Hg(II)-dependent inactivation of Sod and Pcat. Strains lacking Sod or Pcat have increased levels of oxidized BSH. Reduced BSH is necessary to buffer both cytosolic Hg(II) and ROS. In the absence of reduced BSH, Hg(II) accumulation inactivates enzymes, such as aconitase, with solvent accessible Fe-S clusters and increases intracellular free Fe. The increased free Fe(II) participates in Fenton chemistry resulting in an increase in hydroxyl radicals causing DNA damage. Thus, exposure to Hg(II) results in oxidative stress even though Hg(II) is not a redox active metal and mutations that diminish cellular defenses against ROS indirectly increase Hg(II) sensitivity. It is also probable that BSH directly acts as a Hg(II) ligand (19, 34).

Oxidative stress among the prokaryotes has been mostly examined in *E. coli* with little attention to physiologically diverse microbes. *Thermus* spp. inhabit hot environments where heat lowers maximal oxygen saturation (4.53 mg/L at 65 ºC) relative to saturation under conditions utilized to culture *E. coli* (6.73 mg/L at 37 ºC) (35). When tested,

Thermus aquaticus grew better under microaerophilic, as compared to more aerated, conditions correlating with a decreased ability to detoxify ROS (36). These facts may also explain the presence of pseudocatalase rather than catalase (37). Relative to *E. coli*, *T. thermophilus* displays a distinct gene expression pattern upon Hg(II) exposure. In *T. thermophilus*, *sod*, *pcat*, *osmC* and *tlpA* transcripts, but not *bcp,* were induced in response to Hg(II) (Fig. 1A). In *E. coli*, Hg(II) was found to induce the expression of *sodB* and the peroxiredoxin *ahpC*, but not *katG* and *katE* that encode catalases (38). The *E. coli sodA*, which is the *T. thermophilus sod* orthologue, was repressed by short term Hg(II) exposure (38). We previously showed that *E. coli* and *T. thermophilus* differentially regulate the transcription of genes required for LMW-thiol synthesis upon Hg(II) exposure (19). Taken together, these findings highlight the fact that these two bacteria, one deep branching and the other highly derived, differ in their responses to Hg(II). The findings reported here, therefore, provide a foundation for future studies to decipher how microbial systems have evolved in response to the combined toxic effects of metals and oxygen.

The amount of BSH in *T. thermophilus* cells appears to be lower than the concentration of glutathione typically found in Gram-negative bacteria. Assuming that *T. thermophilus* cells have the same volume and dry weight as *E. coli* cells, the cytosolic concentration of BSH would be ~40 μM under the growth condictions utilized. Previous work found the concentration of BSH in *Bacillus subtilis* and *Deinococcus radiodurans* to be ~200 μM (39). The concentration of glutathione in *E. coli* cells is ~5 mM (39). The lower concentration of BSH in *T. thermophilus* cells could constrain the ability to use BSH to buffer against ROS when Hg(II) accumulates in the cytosol. This could result in an increased reliance on alternative ROS mitigating factors, such as Sod, to protect the cell.

BSH pools were decreased by incubation with Hg(II) (19) and in mutant strains lacking Pcat or Sod. We found that BSH functions to prevent ROS poisoning in *T. thermophilus* (Fig. S1). The Δ*sod* and Δ*pcat* strains had lower levels of reduced BSH, but the same overall concentration of BSH (Fig. 3A) suggesting that ROS or a byproduct of ROS metabolism results in increased BSH oxidation. A role for BSH as a buffer against ROS accumulation could explain why there was no detectable difference in ROS titers in the Δ*sod*, Δ*pcat*, and WT strains in absence of Hg(II). It is currently unknown which enzyme(s) is (are) responsible for reducing BSSB back to BSH in *T. thermophilus*. In yeast and protists glutathione reductase is inhibited by Hg(II) (40, 41) and if *T. thermophilus* utilizes a similar enzyme to reduce BSSB, which is likely, it is possible that this enzyme is also inhibited by Hg(II), resulting in a decreased ability to recycle BSSB to BSH (Fig. 5). It was hypothesized that YpdA functions as a BSSB reductase in *B. subtilis* (42). The genome of *T. thermophilus* encodes for a gene product that is 39% identical to YpdA (YP_144481). Future studies will be necessary to determine the effect of this gene product on BSSB recycling.

In some cyanobacteria, glutaredoxin reductase posses a mercuric reductase activity (43) and it is thus conceivable that MerA in *Thermus* may serve as a BSSB reductase. This possibility is hard to evaluate with our current mechanistic understanding of MerA, which is largely based on studies with proteobacterial reductases (44, 45). MerA in *Thermus* is a core MerA, lacking the 70 amino acids N-terminus (NmerA) (46) that functions in delivering S-Hg-S to the redox active site of the enzyme (45), and thus must differ from the full length proteobacterial variants in its interaction with its substrates . We

322 also found that the reduced BSH pool in the Δ*merA* strain was similar to that of the WT
323 (not shown).
324 We previously reported the high concentrations of sulfides in strain HB27 (324.1±
325 88.4 nmol/g dry weight) (19). The natural habitats for *Thermus* spp. are usually moderate
326 to high temperature terrestrial springs with low sulfide and circumneutral to alkaline pH
327 suggesting a chemoorganotrophic metabolism (47, 48). However, genome sequences of
328 several *Thermus* spp., including HB27, revealed presence of genes related to the SOX
329 and PSR system (49). These systems may specify, respectively, mixotrophic growth with
330 reduced sulfur as an energy source and anaerobic polysulfide respiration (50). We are
331 not aware of reports demonstrating such metabolic capabilities in *Thermus*, and our
332 findings in this and our previous (19) papers highlight the need for further research on this
333 topic.
334 Hg(II) readily reacts with sulfide to form HgS and evidence suggests that sulfide
335 production could be a Hg(II) detoxification mechanism (51). We did not notice a significant
336 decrease in the size of the sulfide pool upon challenge with Hg(II) (19); however, the small
337 amount of Hg(II) added to *T. thermophilus* cultures relative to the size of the sulfide pool
338 likely render it impossible to detect a decline in sulfide concentration upon Hg(II) binding.
339 Hydrogen sulfide has been found to aid in the detoxification of ROS (52-54). In the future
340 we would like to decrease the size of the sulfide pool and examine the consequences on
341 ROS metabolism and Hg(II) challenge.
342 Hg(II) inhibited Sod, Pcat, and AcnA *in vivo* and *in vitro*, but a higher concentration
343 of Hg(II) was required to inhibit these enzymes *in vitro*. Moreover, the concentrations of
344 Hg(II) necessary to inhibit SOD and Pcat *in vitro* were much higher than predicted to

accumulate inside cells under the growth conditions utilized. Among the scenarios that could explain this discrepancy, the most plausible explanation might be the difference in available Hg(II) *in vivo* and *in vitro.* Mercury bioavailability is greatly affected by the presence of ligands (55-57). If cell lysis during preparation of crude cell extracts releases ligands that are compartmentalized within intact cells, these may greatly reduce Hg(II) bioavailability in *in vitro* assays. This is suggested by our laboratory's protocols for mercuric reductase assays whereby resting cells and crude extract activities are measured at 10 and 100 μM Hg(II) (58), respectively. The high concentrations of sulfide in strain HB27 (19), which are likely present as labile organic and inorganic persulfides and polysulfides (59), may greatly limit Hg(II) bioavailability in crude cell extracts. The precise nature of the intracellular sulfide pool in strain HB27 and how it interacts with metal exposure and other stressors will be an important future avenue of investigation.

This study reports on the effects of Hg(II) on *T. thermophilus*, which belongs to one of the earliest aerobic bacterial lineages. We report that ROS detoxification is important for Hg(II) tolerance; therefore, in *T. thermophilus*, resistance to Hg(II) is achieved through both *mer*-based detoxification (18, 19) and the oxidative stress response. We previously suggested that the *mer* system evolved in response to Earth oxygenation due to the increased availability of oxidized Hg species (46). It is likely that these same environmental changes led to the evolution of the oxidative stress response. While numerous reports have documented metal-induced oxidative stress [reviewed in (10, 60, 61)], few examined how responses to this stress alleviate metal toxicity among prokaryotes. Our findings in *T. thermophilus* alert us to these hitherto little-studied aspects of metal homeostasis.

EXPERIMENTAL PROCEDURES

Chemicals and bacterial growth conditions

Thermus thermophilus HB27 (WT) and its mutants were cultured at 65°C in 461 Castenholz TYE medium (complex medium; CM) (18). When cultured in liquid medium, cells grown in 3 mL of medium in 10 mL test tubes incubated perpendicular, and shaken at 200 rpm. Test tubes were used to grow cells for ROS analysis, RNA extraction, resistance assays, and AP site quantification. Flasks (2:3 gaseous headspace to liquid medium ratio) were used to grow cultures to generate cell free extracts for enzyme assays, zymograms, thiol content determination, and for intracellular Fe-concentration determination. Solid culture medium was supplemented with 1.5% (wt/vol) agar. Kanamycin (Kan) and Hygromycin B were supplemented at 25 μg mL^{-1} and 40 μg mL^{-1}, respectively. Unless otherwise stated, overnight (ON) cultures of *T. thermophilus* were diluted in fresh medium to optical density $(OD)_{600}$ of 0.1 and further grown to OD_{600} of ~0.3 before challenged with toxicants (fosfomycin, paraquat, or $HgCl_2$). Mercury was used as $HgCl_2$ for all assays. Protein concentrations were determined using Bradford procedure (Bio-Rad Laboratories Inc., Hercules, CA).

Mutant construction

The in-frame deletions for *sod* (WP_011172643.1) and *pcat* (WP_011174225.1) were performed as previously described (19). DNA primers used in this study are listed in table S1. Gene replacements were confirmed by DNA sequencing. For genetic complementation, the 16S rRNA gene (*rrsB*: TT_C3024), was replaced with the

complementing gene constructs according to Gregory and Dahlberg (62). All mutant strains used the native gene promoter to express resistance cassettes or genes.

Monitoring reactive oxygen species

The fluorophore 2',7'-dichlorodihydrofluorescein diacetate (H_2DCFDA) (63-65) was used for ROS monitoring. Cells were incubated for 60 minutes in the presence or absence of Hg(II). Cells from 1 mL of culture were pelleted, washed with phosphate buffered saline (PBS), resuspended in 500 µL of 10 µM H_2DCFDA in PBS, and incubated for 30 min at 37°C. After incubation, cells were washed with PBS and lysed by sonication. Fluorescence was measured (Perkin Elmer HTS 7000 Plus Bio Assay Reader) at 485 nm as excitation and 535 nm as emission wavelengths. Data were normalized to protein concentration.

RNA extraction, cDNA synthesis and qPCR

For induction of gene expression, cells were exposed to 1 µM Hg(II) for 15 or 30 min. Three mL aliquots were removed and mixed with RNA protect (QIAGEN). RNA extraction and cDNA synthesis were performed as previously described (19). Transcripts were quantified by qPCR (iCycler iQ, Bio-Rad Laboratories Inc., Hercules, CA) as previously described (19). DNA primers and cycling temperatures used are listed in Table S2.

Enzymatic assays

Cultures (25 mL) were exposed to Hg(II) for 30 minutes, cells pelleted, washed with PBS, and cell pellets were frozen until further use. Crude cell extracts were prepared as

previously described (58). All enzyme assays were performed at 50°C. For exposure of crude cell lystates, Hg(II) was added at the indicated concentrations and incubated for 5 min before measuring enzymatic activity. The assay described by Oberley and Spitz (66) was used to determine SOD activity with 30 µg of crude extract. One unit was defined as the amount of enzyme needed to reduce the reference rate by 50% (66). Measurements were carried out with an AVIV 14 UV-VI spectrophotometer. Catalase activity was measured as described by Beers and Seizer (67) with 0.6 mg of protein extract. One unit was defined as the amount of enzyme needed to degrade 1 µmole of H_2O_2 per min (Ɛ= 43.6 $M^{-1}cm^{-1}$ for H_2O_2). For aconitase activity, cell lysis was performed under anaerobic conditions as described elsewhere (68) with 20 µg of protein extract. One unit was defined as the amount of enzyme needed to degrade one µmole of DL-isocitrate per sec (Ɛ= 3.6 $mM^{-1}cm^{-1}$ for cis-aconitate). To determine the *in vivo* Hg(II)-dependent inhibition of H_2O_2 and superoxide consumptions, protein synthesis was stopped by adding 150 µg chloramphenicol/mL to cells grown to OD_{600} of ~0.3, before 5 µM Hg(II) was added. Cells were incubated for 30 min before harvesting as described above. Catalase and aconitase activities were measured with a UVmini-1240 spectrophotometer (Shimadzu Corp. Kyoto, Japan).

Resistance assays

Overnight cultures were diluted to $O.D_{600}$ 0.1 in fresh CM and various concentrations of toxicant (fosfomycin, paraquat, or $HgCl_2$) were added to individual samples at different concentration ranges. Resistance was assessed as the percentage of growth observed at the indicated times relative to the control that was unexposed to the toxicant (100% of

438 growth). Soft agar assays were used to assess H_2O_2 sensitivity. Cells were grown as for
439 liquid assays and 40 µL of the culture was added to 4 mL of CM soft agar (0.8% wt/vol)
440 and then poured over a 25 mm petri dish with CM agar. Ten µL of 10 mM H_2O_2 was added
441 to the center of the plate. The halo of growth inhibition was measure after 24 hours
442 incubation.
443
444 **Zymograms**
445 SOD and catalase in-gel activities were performed as described elsewhere (69). For SOD
446 and Pcat activities, 25 µg and 50 µg, respectively, of cell lysates were loaded on the gels.
447 Cell lysates were prepared as described for enzymatic assays.
448
449 **Thiol concentration determination**
450 Extraction and quantification of low molecular weight thiols was performed as previously
451 described (19). Briefly cells were resuspended in D-mix (acetonitrile, HEPES, EDTA and
452 mBrB) and incubated for 15 minutes at 60°C in the dark. Free-thiols are complexed with
453 mBrB before the reaction was stopped with methanesulfonic acid. Samples are
454 centrifuged and cell debris was separated from the soluble thiols before quantifying LMW
455 thiols by HPLC. Cell debris was dried to determine the dry weight of cell material derived
456 from each sample. For total BSH determinations, cells were exposed to 10 mM DTT for
457 30 min prior to thiol extraction.
458
459 **Intracellular iron quantification**
460 The assay followed the description of LaVoie *et al*. (21). Cultures (100 mL) were exposed
461 to Hg(II) for 30 min. Cells were pelleted by centrifugation, resuspended in 5 mL of PBS

with 10 mM diethylene triamine pentaacetic acid (DTPA) and 20 mM deferoxamine mesylate salt (DF), shaken at 37 °C for 15 min at 180 rpm, and pelleted at 4°C. Cells were washed once with ice-cold 20 mM Tris–HCl (pH 7.4), resuspended in the same buffer with 15% (v/v) glycerol, and stored at -80 °C. For EPR analysis, cell suspensions were thawed on ice and 200 µL aliquots were dispensed into 4-mm OD quartz EPR tubes and frozen in liquid nitrogen. Continuous-wave (CW) EPR experiments were performed with an X-band Bruker EPR spectrometer (Elexsys580) equipped with an Oxford helium-flow cryostat (ESR900) and an Oxford temperature controller (ITC503). EPR parameters used in our experiments were: microwave frequency, 9.474 GHz; microwave power, 20 mW; modulation amplitude, 2 mT; and sample temperature, 25°K. The Fe(III):DF concentration of each sample was determined by comparing the peak-to-trough height of EPR signal at g = 4.3 against the standard sample with a known Fe(III):DF concentration (50 µM $FeCl_3$ and 20 mM DF in 20 mM Tris–HCl at pH 7.4 with 15% [v/v] glycerol).

Quantification of apurinic or apyrimidinic (AP) sites

Cells were exposed to Hg(II) for 60 min. Three mL of cultures were pelleted and washed with PBS prior to DNA extraction using QIAamp DNA kit (QIAGEN). AP sites were quantified using the Oxiselect™ Oxidative DNA Damage Quantification Kit (Cell Biolabs).

Statistical analysis

One-way ANOVA followed by a Dunnet test analysis was performed for multiple group comparison to a control. For two group comparisons (controls vs treatment), student's t-tests were performed.

Data availability

All data will be provided upon request.

FUNDING

JN was a recipient of a Becas Chile from CONICY, Chile. The Boyd Laboratory is supported by the National Science Foundation grant MCB-1750624. The Barkay Laboratory was supported by the National Science Foundation grant PLR-1304773.

ACKNOWLEDGMENTS

We thank Judy Wall and Tim McDermott for their thoughtful and thorough reviews of this manuscript. Addressing their comments resulted in a greatly strengthened study. We thank Alexei M. Tyryshkin, Ph.D., for his help with the EPR experiments and Akira Nakamura, Ph.D., for kindly providing us with a plasmid harboring the Hygromycin B resistance.

REFERENCES

1. Hartmann RK, Wolters J, Kröger B, Schultze S, Specht T, Erdmann VA. 1989. Does *Thermus* represent another deep Eubacterial branching? Syst Appl Microbiol 11:243-249.
2. Geesey GG, Barkay T, King S. 2016. Microbes in mercury-enriched geothermal springs in western North America. Sci Total Environ 569-570:321-331.
3. Messner KR, Imlay JA. 2002. Mechanism of superoxide and hydrogen peroxide formation by fumarate reductase, succinate dehydrogenase, and aspartate oxidase. J Biol Chem 277:42563-42571.
4. Imlay JA. 2003. Pathways of oxidative damage. Annu Rev Microbiol 57:395-418.
5. Valko M, Morris H, Cronin MTD. 2005. Metals, toxicity and oxidative stress. Curr Med Chem 12:1161-1208.

6. Miller DM, Lund BO, Woods JS. 1991. Reactivity of Hg(II) with superoxide: Evidence for the catalytic dismutation of superoxide by Hg(II). J Biochem Mol Toxicol 6:293-298.
7. Ariza ME, Bijur GN, Williams MV. 1998. Lead and mercury mutagenesis: Role of H_2O_2, superoxide dismutase, and xanthine oxidase. Environ Mol Mutagen 31:352-361.
8. Lund BO, Miller DM, Woods JS. 1991. Mercury-induced H_2O_2 production and lipid peroxidation in vitro in rat kidney mitochondria. Biochem Pharmacol 42 Suppl:S181-187.
9. Ariza ME, Williams MV. 1999. Lead and mercury mutagenesis: Type of mutation dependent upon metal concentration. J Biochem Mol Toxicol 13:107-112.
10. Ercal N, Gurer-Orhan H, Aykin-Burns N. 2001. Toxic metals and oxidative stress part I: mechanisms involved in metal-induced oxidative damage. Curr Top Med Chem 1:529-539.
11. Nath KA, Croatt AJ, Likely S, Behrens TW, Warden D. 1996. Renal oxidant injury and oxidant response induced by mercury. Kidney Int 50:1032-1043.
12. Xu FF, Imlay JA. 2012. Silver(I), mercury(II), cadmium(II), and zinc(II) target exposed enzymic iron-sulfur clusters when they toxify *Escherichia coli*. Appl Environ Microbiol 78:3614-3621.
13. Keyer K, Imlay JA. 1996. Superoxide accelerates DNA damage by elevating free-iron levels. Proc Natl Acad Sci U S A 93:13635-13640.
14. Jang S, Imlay JA. 2007. Micromolar intracellular hydrogen peroxide disrupts metabolism by damaging iron-sulfur enzymes. J Biol Chem 282:929-937.
15. Imlay JA, Chin SM, Linn S. 1988. Toxic DNA damage by hydrogen peroxide through the Fenton reaction in vivo and in vitro. Science 240:640-642.
16. Barkay T, Miller SM, Summers AO. 2003. Bacterial mercury resistance from atoms to ecosystems. FEMS Microbiol Rev 27:355.
17. Boyd ES, Barkay T. 2012. The mercury resistance operon: from an origin in a geothermal environment to an efficient detoxification machine. Front Microbiol 3:349.
18. Wang Y, Freedman Z, Lu-Irving P, Kaletsky R, Barkay T. 2009. An initial characterization of the mercury resistance (*mer*) system of the thermophilic bacterium *Thermus thermophilus* HB27. FEMS Microbiol Ecol 67:118.
19. Norambuena J, Wang Y, Hanson T, Boyd JM, Barkay T. 2018. Low molecular weight thiols and thioredoxins are important players in Hg(II) resistance in *Thermus thermophilus* HB27. Appl Environ Microbiol 84:e01931-17.
20. Oram PD, Fang X, Fernando Q, Letkeman P, Letkeman D. 1996. The formation of constants of mercury(II)--glutathione complexes. Chem Res Toxicol 9:709-712.
21. LaVoie SP, Mapolelo DT, Cowart DM, Polacco BJ, Johnson MK, Scott RA, Miller SM, Summers AO. 2015. Organic and inorganic mercurials have distinct effects on cellular thiols, metal homeostasis, and Fe-binding proteins in *Escherichia coli*. J Biol Inorg Chem 20:1239-1251.
22. Murphy Michael P. 2009. How mitochondria produce reactive oxygen species. Biochem J 417:1-13.
23. Hidalgo A, Betancor L, Moreno R, Zafra O, Cava F, Fernandez-Lafuente R, Guisan JM, Berenguer J. 2004. *Thermus thermophilus* as a cell factory for the production

of a thermophilic Mn-dependent catalase which fails to be synthesized in an active form in *Escherichia coli*. Appl Environ Microbiol 70:3839-3844.
24. Clarke DJ, Ortega XP, Mackay CL, Valvano MA, Govan JR, Campopiano DJ, Langridge-Smith P, Brown AR. 2010. Subdivision of the bacterioferritin comigratory protein family of bacterial peroxiredoxins based on catalytic activity. Biochemistry 49:1319-1330.
25. Flohe L, Toppo S, Cozza G, Ursini F. 2011. A comparison of thiol peroxidase mechanisms. Antioxid Redox Signal 15:763-780.
26. Achard ME, Hamilton AJ, Dankowski T, Heras B, Schembri MS, Edwards JL, Jennings MP, McEwan AG. 2009. A periplasmic thioredoxin-like protein plays a role in defense against oxidative stress in *Neisseria gonorrhoeae*. Infect Immun 77:4934-4939.
27. Gaballa A, Newton GL, Antelmann H, Parsonage D, Upton H, Rawat M, Claiborne A, Fahey RC, Helmann JD. 2010. Biosynthesis and functions of bacillithiol, a major low-molecular-weight thiol in Bacilli. Proc Natl Acad Sci U S A 107:6482-6486.
28. Chi BK, Gronau K, Mäder U, Hessling B, Becher D, Antelmann H. 2011. S-Bacillithiolation protects against hypochlorite stress in *Bacillus subtilis* as revealed by transcriptomics and redox proteomics. Mol Cell Proteomics 10:M111.009506.
29. Woodmansee AN, Imlay JA. 2002. Quantitation of intracellular free iron by electron paramagnetic resonance spectroscopy. Methods Enzymol 349:3-9.
30. de Mello Filho AC, Meneghini R. 1985. Protection of mammalian cells by o-phenanthroline from lethal and DNA-damaging effects produced by active oxygen species. Biochim Biophys Acta 847:82-89.
31. Kanno S, Iwai S, Takao M, Yasui A. 1999. Repair of apurinic/apyrimidinic sites by UV damage endonuclease; a repair protein for UV and oxidative damage. Nucleic Acids Res 27:3096-3103.
32. Kidane D, Murphy DL, Sweasy JB. 2014. Accumulation of abasic sites induces genomic instability in normal human gastric epithelial cells during *Helicobacter pylori* infection. Oncogenesis 3:e128.
33. Morita R, Nakane S, Shimada A, Inoue M, Iino H, Wakamatsu T, Fukui K, Nakagawa N, Masui R, Kuramitsu S. 2010. Molecular mechanisms of the whole DNA repair system: A comparison of bacterial and eukaryotic systems. J Nucleic Acids 2010:179594.
34. Rosario-Cruz Z, Boyd JM. 2015. Physiological roles of bacillithiol in intracellular metal processing. Curr Genet 62:59-65.
35. Mortimer CH. 1981. The oxygen content of air-saturated fresh waters over ranges of temperature and atmospheric pressure of limnological interest. Int Ver Theor Angew 22:1-23.
36. Allgood GS, Perry JJ. 1986. Characterization of a manganese-containing catalase from the obligate thermophile *Thermoleophilum album*. J Bacteriol 168:563-567.
37. Whittaker MM, Barynin VV, Antonyuk SV, Whittaker JW. 1999. The oxidized (3,3) state of manganese catalase. Comparison of enzymes from *Thermus thermophilus* and *Lactobacillus plantarum*. Biochemistry 38:9126-9136.
38. Onnis-Hayden A, Weng H, He M, Hansen S, Ilyin V, Lewis K, Guc AZ. 2009. Prokaryotic real-time gene expression profiling for toxicity assessment. Environ Sci Technol 43:4574-4581.

39. Newton GL, Rawat M, La Clair JJ, Jothivasan VK, Budiarto T, Hamilton CJ, Claiborne A, Helmann JD, Fahey RC. 2009. Bacillithiol is an antioxidant thiol produced in Bacilli. Nat Chem Biol 5:625-627.
40. Picaud T, Desbois A. 2006. Interaction of glutathione reductase with heavy metal: The binding of Hg(II) or Cd(II) to the reduced enzyme affects both the redox dithiol pair and the flavin. Biochemistry 45:15829-15837.
41. Shigeoka S, Onishi T, Nakano Y, Kitaoka S. 1987. Characterization and physiological function of glutathione reductase in *Euglena gracilis* z. Biochem J 242:511-515.
42. Helmann JD. 2011. Bacillithiol, a new player in bacterial redox homeostasis. Antioxid Redox Signal 15:123-33.
43. Marteyn B, Sakr S, Farci S, Bedhomme M, Chardonnet S, Decottignies P, Lemaire SD, Cassier-Chauvat C, Chauvat F. 2013. The *Synechocystis* PCC6803 MerA-like enzyme operates in the reduction of both mercury and uranium under the control of the glutaredoxin 1 enzyme. J Bacteriol 195:4138.
44. Ledwidge R, Patel B, Dong A, Fiedler D, Falkowski M, Zelikova J, Summers AO, Pai EF, Miller SM. 2005. NmerA, the metal binding domain of mercuric ion reductase, removes Hg^{2+} from proteins, delivers it to the catalytic core, and protects cells under glutathione-depleted conditions. Biochemistry 44:11402-11416.
45. Lian P, Guo HB, Riccardi D, Dong A, Parks JM, Xu Q, Pai EF, Miller SM, Wei DQ, Smith JC, Guo H. 2014. X-ray structure of a Hg^{2+} complex of mercuric reductase (MerA) and quantum mechanical/molecular mechanical study of Hg^{2+} transfer between the C-terminal and buried catalytic site cysteine pairs. Biochemistry 53:7211-7222.
46. Barkay T, Kritee K, Boyd E, Geesey G. 2010. A thermophilic bacterial origin and subsequent constraints by redox, light and salinity on the evolution of the microbial mercuric reductase. Environ Microbiol 12:2904-2917.
47. Brock TD. 1981. Extreme thermophiles of the genera *Thermus* and *Sulfolobus.* The Prokaryotes pp 978-984
48. Kristjansson JK, Alfredsson GA. 1983. Distribution of *Thermus* spp. in Icelandic hot springs and a thermal gradient. Appl Environ Microbiol 45:1785-1789.
49. Murugapiran SK, Huntemann M, Wei C-L, Han J, Detter JC, Han C, Erkkila TH, Teshima H, Chen A, Kyrpides N, Mavrommatis K, Markowitz V, Szeto E, Ivanova N, Pagani I, Pati A, Goodwin L, Peters L, Pitluck S, Lam J, McDonald AI, Dodsworth JA, Woyke T, Hedlund BP. 2013. *Thermus oshimai* JL-2 and *T. thermophilus* JL-18 genome analysis illuminates pathways for carbon, nitrogen, and sulfur cycling. Stand Genomic Sci 7:449-468.
50. Jormakka M, Yokoyama K, Yano T, Tamakoshi M, Akimoto S, Shimamura T, Curmi P, Iwata S. 2008. Molecular mechanism of energy conservation in polysulfide respiration. Nat Struct Mol Biol 15:730-737.
51. Glendinning KJ, Macaskie LE, Brown NL. 2005. Mercury tolerance of thermophilic *Bacillus* sp. and *Ureibacillus* sp. Biotechnol Lett 27:1657-1662.
52. Spassov SG, Donus R, Ihle PM, Engelstaedter H, Hoetzel A, Faller S. 2017. Hydrogen sulfide prevents formation of reactive oxygen species through PI3K/Akt

signaling and limits ventilator-induced lung injury. Oxid Med Cell Longev 2017:3715037.
53. Chang L, Geng B, Yu F, Zhao J, Jiang H, Du J, Tang C. 2008. Hydrogen sulfide inhibits myocardial injury induced by homocysteine in rats. Amino Acids 34:573-585.
54. Geng B, Chang L, Pan C, Qi Y, Zhao J, Pang Y, Du J, Tang C. 2004. Endogenous hydrogen sulfide regulation of myocardial injury induced by isoproterenol. Biochem Biophys Res Commun 318:756-763.
55. Hsu-Kim H, Kucharzyk KH, Zhang T, Deshusses MA. 2013. Mechanisms regulating mercury bioavailability for methylating microorganisms in the aquatic environment: a critical review. Environ Sci Technol 47:2441-2456.
56. Barkay T, Gillman M, Turner RR. 1997. Effects of dissolved organic carbon and salinity on bioavailability of mercury. Appl Environ Microbiol 63:4267-4271.
57. Farrell RE, Germida JJ, Huang PM. 1993. Effects of chemical speciation in growth media on the toxicity of mercury(II). Appl Environ Microbiol 59:1507-1514.
58. Vetriani C, Chew YS, Miller SM, Yagi J, Coombs J, Lutz RA, Barkay T. 2005. Mercury adaptation among bacteria from a deep-sea hydrothermal vent. Appl Environ Microbiol 71:220-226.
59. Luebke JL, Shen J, Bruce KE, Kehl-Fie TE, Peng H, Skaar EP, Giedroc DP. 2014. The CsoR-like sulfurtransferase repressor (CstR) is a persulfide sensor in *Staphylococcus aureus*. Mol Microbiol 94:1343-1360.
60. Nies DH. 1999. Microbial heavy-metal resistance. Appl Microbiol Biotechnol 51:730-750.
61. Hobman JL, Crossman LC. 2015. Bacterial antimicrobial metal ion resistance. J Med Microbiol 64:471-497.
62. Gregory ST, Dahlberg AE. 2009. Genetic and structural analysis of base substitutions in the central pseudoknot of *Thermus thermophilus* 16S ribosomal RNA. RNA 15:215-223.
63. Wang H, Joseph JA. 1999. Quantifying cellular oxidative stress by dichlorofluorescein assay using microplate reader. Free Radic Biol Med 27:612-616.
64. Myhre O, Andersen JM, Aarnes H, Fonnum F. 2003. Evaluation of the probes 2′,7′-dichlorofluorescin diacetate, luminol, and lucigenin as indicators of reactive species formation. Biochemical Pharmacology 65:1575-1582.
65. Rosario-Cruz Z, Chahal HK, Mike LA, Skaar EP, Boyd JM. 2015. Bacillithiol has a role in Fe-S cluster biogenesis in *Staphylococcus aureus*. Mol Microbiol 98:218-242.
66. Spitz DR, Oberley LW. 1989. An assay for superoxide dismutase activity in mammalian tissue homogenates. Anal Biochem 179:8-18.
67. Beers RF, Jr., Sizer IW. 1952. A spectrophotometric method for measuring the breakdown of hydrogen peroxide by catalase. J Biol Chem 195:133-140.
68. Mashruwala AA, Boyd JM. 2017. The *Staphylococcus aureus* SrrAB regulatory system modulates hydrogen peroxide resistance factors, which imparts protection to aconitase during aerobic growth. PLoS One 12:e0170283.
69. Weydert CJ, Cullen JJ. 2010. Measurement of superoxide dismutase, catalase and glutathione peroxidase in cultured cells and tissue. Nat Protoc 5:51-66.

695

696

697

Figures

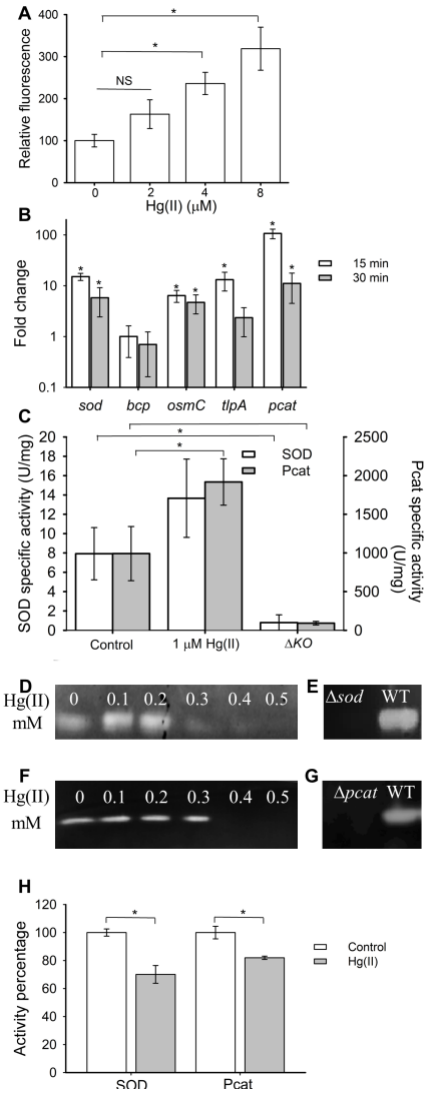

Figure 1. Mercury exposure induces ROS, increases Sod and Pcat expresion, and inhibits SOD and Pcat activities. (A) Cultures of *T. thermophilus* (WT) were exposed to varying concentrations of Hg(II) for 60 minutes before total ROS was measured using H_2DCFDA. (B) Induction of superoxide dismutase (*sod*), bacterioferritin comigratory protein (*bcp*), organic hydroperoxide reductase (*osmC*), thiol peroxidase (*tlpA*) and pseudocatalase (*pcat*) transcription, was measured in the WT strain after 15 or 30 minutes of exposure to 1 μM of Hg(II). (C) WT cells were exposed to 0 or 1 μM of Hg(II)

for 30 minutes and superoxide (white) and H_2O_2 (grey) consumption was monitored. Each activity was compared to activity of the respective Δ*sod* or Δ*pcat* mutant strains (indicated as Δ*KO* in the figure) not exposed to Hg(II). (D-G) Crude protein extracts of the WT strain where incubated with different Hg(II) concentrations. Qualitative zymograms where revealed for (D and E) SOD activity or (F and G) Pcat activity. Cell extracts of the (E) WT and Δ*sod* strains or (G) WT and Δ*pcat* are also shown. (H) WT cells were exposed to 150 µg/mL of chloramphenicol and incubated for 30 min with 0 (white) or 5 µM of Hg(II) (grey); superoxide (SOD) and H_2O_2 (Pcat) consumption were monitored and activity percentages (relative to the unexposed strain [control]) are shown. For panels A, B, and C, each point represents the average of at least three independent experiments and standard deviations are shown. For panel H, 3 replicate experiments are shown. Student's t-tests were performed on the data in panels A and C, and * indicates $P \leq 0.05$. A Mann-Whitney Rank Sum Test was performed on the data in panel B and * $P \leq 0.05$**.** NS denotes not significant.

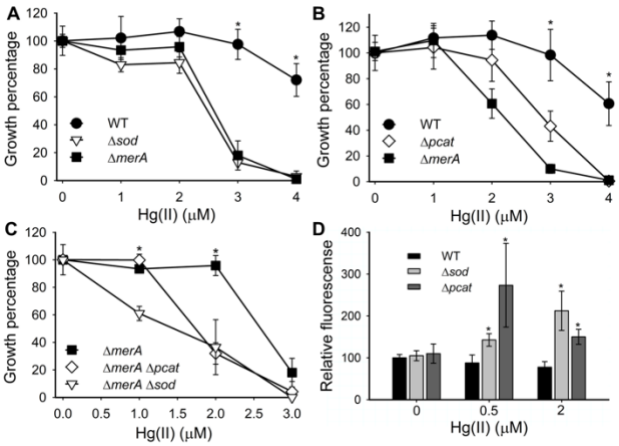

Figure 2. *T. thermophilus* strains lacking superoxide- or H_2O_2-scavenging activities are more sensitive to Hg(II) and have increased ROS levels upon Hg(II) exposure. Culture optical densities were determined after 21 hours (A and C) or 18 hours (B) of growth. Growth in the unexposed control was considered 100% of growth. (D) Cultures were grown and one-half of each was exposed to Hg(II) for 60 minutes before ROS were quantified using DCFDA. The fluorescence obtained for the unexposed WT strain was considered 100% fluorescence. Each point represents the average of three independent cultures and standard deviations are shown. Student's t-tests were performed and * indicates a $P \leq 0.05$.

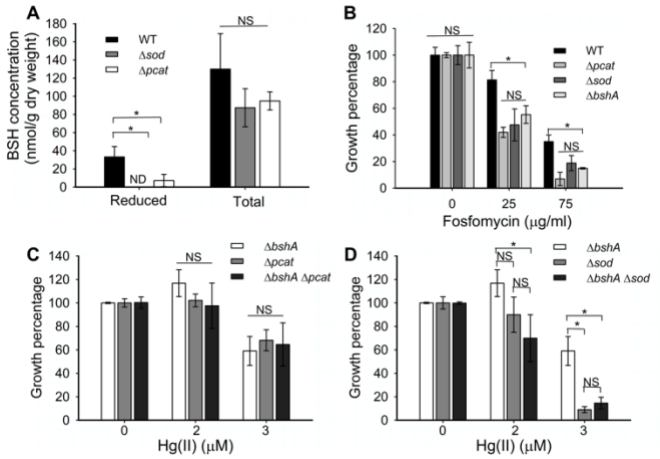

734

735 **Figure 3. *T. thermophilus* strains lacking Sod or Pcat have decreased levels of**
736 **reduced BSH pools.** (A) Cultures were grown to an OD_{600} of 0.3 and exposed, or not, to
737 10 mM DTT for 30 minutes before LMW thiols were quantified with mBrB. DTT treated
738 cells were used to measure total BSH. (B) Final culture optical densities were recorded
739 after 20 hours of growth in cultures exposed to various concentration of fosfomycin. (C)
740 Effect of Hg(II) on cell growth was evaluated after 20 hours of growth in the Δ*pcat*, Δ*bshA*,
741 and Δ*pcat* Δ*bshA* strains and (D) in the Δ*sod*, Δ*bshA*, and Δ*sod* Δ*bshA* strains. Unexposed
742 controls were considered 100% of growth. Each point represents the average of three
743 independent cultures and standard deviations are shown. Student's t-tests were
744 performed on the data and * indicates a $P \leq 0.05$. NS denotes not significant and ND
745 denotes no signal detected.

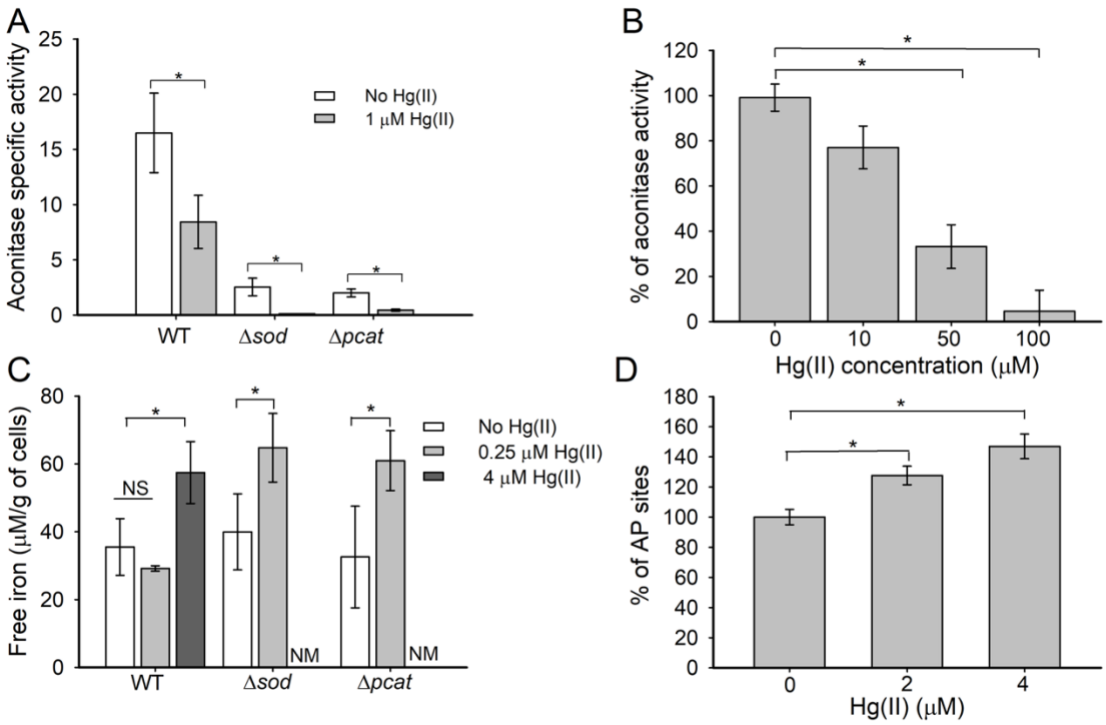

746

747 **Figure 4. Hg(II) stress results in aconitase inactivation, increased intracellular free**
748 **iron, and DNA damage.** (A) Aconitase activity was monitored in cell free lysates after
749 whole cells had been exposed, or not, to 1μM Hg(II) for 30 minutes. (B) Cell-free lysates
750 from the WT strain were exposed to 0-100 μM Hg(II) before aconitase activity was
751 determined. (C) The concentration of free Fe was quantified after exposure to 0.25 μM
752 Hg(II) or to 4 μM Hg(II) for 30 minutes. Cell weight is reported as wet weight. (D) DNA
753 damage was determined by quantifying the number of apurinic/apyrimidinic sites (AP
754 sites) in the WT strain (cells unexposed to Hg(II) had an average of 8.38±0.77 AP sites
755 per 100,000 base-pairs of DNA). Each point represents the average of at least three
756 independent cultures and standard deviations are shown. Where shown, student's t-
757 tests were conducted on the data and * indicates $P \leq 0.05$. NS denotes not significant
758 and NM denotes not measured.

759

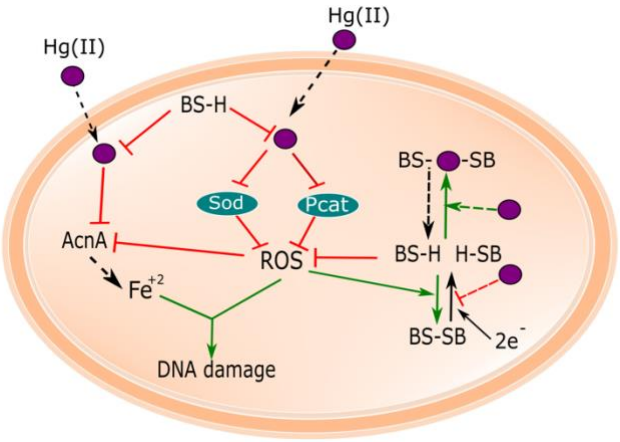

Figure 5. Working model for ROS generation by Hg(II). Exposure of *T. thermophilus* to Hg(II) (purple) results in the inactivation of two ROS detoxifying enzymes (Sod and Pcat) and ROS accumulation. Hg(II) decreases bioavailable BSH, which is necessary to prevent Hg(II) intoxication and ROS accumulation. The presence of Sod and Pcat are necessary to maintain reduced BSH pools, as well as metabolize superoxide and H_2O_2, respectively. Hg(II) accumulation inactivates enzymes, such as aconitase, with solvent accessible Fe-S clusters and increases intracellular free Fe. The free Fe^{2+} participates in Fenton chemistry producing hydroxyl radicals, which damage DNA. Systems inhibited are shown in red and systems favored upon Hg(II) toxicity are shown in green.

Supplementary Material Figure Legends and Tables:

Figure S1. Δ*sod,* Δ*pcat* and Δ*bshA* strains are more sensitive to ROS than the WT strain and Pcat is inhibited by Hg(II). (A) The WT, Δ*sod,* and Δ*bshA* strains were grown with and without paraquat and culture optical densities after 18 hours of growth are shown. Growth in the unexposed control was considered 100% of growth. (B) The zone

778 of clearing monitored after exposure to 10 mM H_2O_2 was evaluated on soft agar plates.
779 (C) Cell-free lysates from the WT strain were exposed to 0-100 µM Hg(II) before catalase
780 activity was determined. Each point represents the average of three independent cultures
781 and standard deviations are shown. Student's t-tests were performed on the data and *
782 indicates P ≤0.05.
783
784 **Figure S2. Genetic complementation of Δ*sod* and Δ*pcat* strains.** (A) Zymogram
785 showing superoxide consumption activity in cell lysates from the WT, Δ*sod*, and
786 complemented Δ*sod rrsB ::sod* (*rrsB*::*sod* in the figure) strains. (B) Zymogram showing
787 hydrogen peroxide consumption activity of cell free lysates from the WT, Δ*pcat*, and
788 complemented Δ*pcat rrsB*::*pcat* (*rrsB*::*pcat* in the figure) strains. (C) Hg(II) resistance for
789 WT, Δ*sod* and *rrsB ::sod* (*rrsB*::*sod* in the figure) and (D) WT, Δ*pcat* and *rrsB*::*pcat*
790 (*rrsB*::*pcat* in the figure). Culture optical densities were determined after 21 hours of
791 growth. Growth in the unexposed control was considered 100% of growth. Pictures of
792 zymograms are representative of three independent experiments. Each point represents
793 the average of three independent experiments and standard deviations are shown.
794 Student's t-tests were performed on the data and * indicates P ≤0.01 when compared to
795 the WT.
796
797 **Figure S3. A Δ*nfo* strain is more sensitive to Hg(II) than the WT.** Strains were cultured
798 with various concentrations of Hg(II) and final optical densities were measured after 20
799 hours. Growth in the unexposed control was considered 100% of growth. Each point
800 represents the average of at least three independent cultures, and bars represent

801 standard deviations. Student's t-tests were performed against the WT strain and *
802 denotes P ≤0.001.
803
804
805

Table S1 Primers and conditions used for qPCR.

Primer	Sequence	C* (µM)	T (°C)	Size (bp)	Source
gyrase-F	GGGCGAGGTCATGGGC	1	61	134	Norambuena et al 2018
gyrase-R	CGCCGTCTATGGAGCCG	0.25			
SOD-F	CGTTCAAGCTTCCTGACCTAGG	1.25	59	117	this study
SOD-R	CGTTGAGGTTCGTCACGTAGGC	1.25			
osmC-F	GATTGAGCTTCTGACCGAGGC	1.25	60	126	this study
osmC-R	AGGACGATCTCCTTCACCCC	1.25			
bcp-F	GAAGTACGGCCTGAACTTTCC	1.25	58	132	this study
bcp-R	TCTATGAGGAAGGTCTGGCG	1.25			
TplA-F	TGGCTTTGTCTTGGAGAACGC	1.25	60	141	this study
TplA-R	CAGAGGTGTTTGGGCAAGGC	1.25			
pcat rev	CGCCACCAGCTCAATGT	1.25	57	105	this study
pcat for	ATGTACCAGTCCTTCAACTTCC	1.25			

*C indicates final concentration of the primers

809 **Table S2** PCR Primers used to construct mutant strains.
810

KO strain	Primer	Sequence
Δ*sod*	1 fum ecoRi for	TCGCGGGAATTCAGGGGAAC
	E HTK SOD rev	ATTGGTCCTTTCATACTTCACCTCCGC
	A sod HTK for	GGAAGCGGAGGTGAAGTATGAAAGGACCAATAATAA
	B sod htk rev	GCTATAAGGCTATGGGGATCAAAATGGTATGCGTT
	4 sod bamh1 rev	GGCGGATCCGGGCCTTA
	F HTK SOD for	GCATACCATTTTGATCCCCATAGCCTTATAGC
	5 fum upins for	GGAAGGTCAACCCCACCCAG
	6 sod downins rev	AAGGCCCTCCTCTTCGGC
Δ*pcat*	A cat	AAAGGAGGGAGAAGATGAAAGGACCAATAATAATG
	B cat	GCCAGGCTAAGGGTCAAAATGGTATGCGTTT
	NdeI 1 cat	GGGCCACATATGCCCAGAAG
	E cat	TTATTGGTCCTTTCATCTTCTCCCTCCTTTC
	F cat	TACCATTTTGACCCTTAGCCTGGCCCGTAG
	4.3 cat ecoR1	CCCAAGCCCGAATTCTTTCCC
	5 cat	ACCCAGGTGTCCTCGAGG
	6 cat	CTGGACCGGGTCTACCCC
Δ*pcat hygB*	NdeI 1 cat	GGGCCACATATGCCCAGAAG
	E cat hygB KO rev	AGGCTTTTTCATCTTCTCCCTCCTTTCG
	B cat hygB KO rev	AGGCTAAGGGCTATTCCTTTGCCCTC
	A cat hygB KO for	GAGGGAGAAGATGAAAAAGCCTGAACTCA
	4.3 cat eco R1	CCCAAGCCCGAATTCTTTCCC
	F cat hygB KO for	AAAGGAATAGCCCTTAGCCTGGCCC

Δ*sod hygB*	1 fum ecoRi for	TCGCGGGAATTCAGGGGAAC
	E sod hygB rev	TTCAGGCTTTTTCATACTTCACCTCCGCTTC
	A sod hygB for	CGGAGGTGAAGTATGAAAAAGCCTGAACTCAC
	B sod hygB rev	GCTATGGGGACTATTCCTTTGCCCTCG
	F sod hygB for	GCAAAGGAATAGTCCCCATAGCCTTATAGCC
	4 SOD HygB rev hindIII	GCCTGAAGCTTGCGGTGG
Δ*nfo*	p1 ecoR1 nfo	GGCCTGGTGGAATTCCGCAAC
	E nfo Htk rev	TGGTCCTTTCATCCCCCGAAGCCTACCACAGG
	B nfo HTk	GGGCGCTCAAAATGGTATGCGTTTTG
	A nfo htk	TGGTAGGCTTCGGGGGATGAAAGGACCAATAATAATG
	p4 bamhI nfo	CCGGGATCCTGGTGAACCTG
	F nfo for	ACGCATACCATTTTGAGCGCCCCACCC
	p5 nfo	CCGTCCTCGTCTACCTCCTG
	p6 nfo	GGAGGATAGATGGGCACGG
rrsB::*pcat*	1.2 ecori Hp 16S for	GTCCGGGGGGAATTCGAGGAGC
	E cat::16S	GAATAAGCCAGGATTTCAAGATGGGGGCATGGACCTCC
	G cat::16S for	ATGCCCCCATCTTGAAATCCTGGCTTATTCTAGCGCC
	H cat::16S rev	AGGCTTTTTCATTTACTTGGCCTTCTCG
	A hygB cat::16S for	GCCAAGTAAATGAAAAAGCCTGAACTCACCG
	B hygB cat::16S rev	TCGAGGAAGTCCATCTATTCCTTTGCCCTCGG
	F cat::16S rev	GCAAAGGAATAGATGGACTTCCTCGAGGCCCTTTC
	4 HindIII 16S rev	CTGCGAAAAGAAGCTTCTCCC
rrsB::*sod*	1.2 ecori Hp 16S for	GTCCGGGGGGAATTCGAGGAGC
	E SOD::16S rev	CTTGCCGCTCAAGATGGGGGCATGG
	G SOD::16S rev	CCCCATCTTGAGCGGCAAGGGGCTTTGTGAGG
	H SOD::16S rev	CTTTTTCATTCAGGCCTTCTTGAAGAACTCC
	A hygB SOD::16S for	CAAGAAGGCCTGAATGAAAAAGCCTGAACTCACCG

	B hygB sod::16S rev	TCGAGGAAGTCCATCTATTCCTTTGCCCTCGG
	F sod::16S rev	GCAAAGGAATAGATGGACTTCCTCGAGGCCCTTTC
	4 HindIII 16S rev	CTGCGAAAAGAAGCTTCTCCC

[1]Underlined sequences indicate restriction enzyme cutting sites.